

Dehydration and Crystallization of Trehalose and Sucrose Glasses Containing Carbonmonoxy-Myoglobin

Fabio Librizzi, Eugenio Vitrano, and Lorenzo Cordone

Dipartimento di Scienze Fisiche ed Astronomiche, Università di Palermo and Istituto Nazionale di Fisica della Materia, 90123 Palermo, Italy

ABSTRACT We report a study wherein we contemporarily measured 1) the dehydration process of trehalose or sucrose glasses embedding carbonmonoxy-myoglobin (MbCO) and 2) the evolution of the A substates in saccharide-coated MbCO. Our results indicate that microcrystallization processes, sizeably different in the two saccharides, take place during dehydration; moreover, the microcrystalline structure is maintained unless the dry samples are equilibrated with a humidity $\geq 75\%$ ($\geq 60\%$) at 25°C for the trehalose (sucrose) sample. The evolution of the parameters that characterize the A substates of MbCO indicates that 1) the effects of water withdrawal are analogous in samples dried in the presence or in the absence of sugars, although much larger effects are observed in the samples without sugar; 2) the distribution of A substates is determined by the overall matrix structure and not only by the sample water content; and 3) the population of A_0 substate (i.e., the substate currently put in relation with MbCO molecules having the distal histidine out of the heme pocket) is largely enhanced during the dehydration process. However, after rehumidification its population is largely decreased with respect to the values obtained, at similar water content, during the first dehydration run.

INTRODUCTION

Some organisms can survive conditions of extreme dehydration and high temperature ($>60^\circ\text{C}$), without suffering any damage. These organisms can remain in the absence of metabolic processes (anhydrobiosis) for several years and recover their vegetative cycle upon rehydration. A characteristic common to these organisms in the dry state is the presence of large concentrations of sugars, particularly trehalose (a disaccharide composed of two $[1 \rightarrow 1]$ -linked α, α units of glucopyranose), which has been found to be the most active saccharide for the preservation of biostructures (see, e.g., Crowe et al., 1996; Panek, 1995; Leslie et al., 1995; Uritani et al., 1995; Prestrelski et al., 1993).

The properties that make trehalose unique with respect to other saccharides for preservation of dry biomaterials are still poorly understood. Recently it has been suggested that the saccharide can be stabilized by incorporating traces of water into the crystalline dihydrate; this would prevent water from acting as a “plasticizer” of the amorphous state (Aldous et al., 1995), thus increasing the glass transition temperature (T_g) of the system (Green and Angell, 1989; Crowe et al., 1996). According to this suggestion a suitable study of the dehydration of the biomolecule-water-sugar glass could give information on the possible microcrystallization and on the “adaptation” of the biostructure. We therefore performed this study wherein we contemporarily measured 1) the dehydration process of trehalose or sucrose glasses embedding carbonmonoxy-myoglobin (MbCO), 2) the dehydration of the same samples after rehumidification,

and 3) the evolution of the A substates (Ansari et al., 1987) in saccharide-coated MbCO, as a function of the water content of the samples. A sample of MbCO in the absence of sugar was also studied for the sake of comparison.

As it is well known (Makinen et al., 1979; Caughey et al., 1981), the CO stretching in MbCO exhibits, in the region $1900 \div 2000 \text{ cm}^{-1}$, four absorption bands, named in order of decreasing wavenumber A_0 , A_1 , A_2 , and A_3 (Ansari et al., 1987). However, due to its low intensity, the A_2 band is usually neglected in the analysis (see, e.g., Mourant et al., 1993). These bands reflect four different conformational substates of MbCO (taxonomic substates) (Frauenfelder et al., 1991) and their relative intensity depends on external parameters such as pH, temperature, and pressure (Ansari et al., 1987; Frauenfelder et al., 1990). Moreover, as shown in Fig. 1, the association band of water is observed adjacent to the CO stretching bands (see, e.g., Eisenberg and Kauzmann, 1969). This band, assigned to a combination of the bending mode of H_2O with intermolecular vibrational modes, in pure liquid water, has its maximum near 2125 cm^{-1} and is the counterpart of the association band in ice (2270 cm^{-1} ; Eisenberg and Kauzmann, 1969).

We obtained qualitative information on the dehydration behavior of our samples by measuring the area delimited by the tangent to the curve at the two minima of the association band, as shown in Fig. 1; moreover, we followed the protein “adaptation” by contemporarily detecting the behavior of the CO stretching bands of MbCO (A substates).

MATERIALS AND METHODS

Horse myoglobin was purchased from Sigma (St. Louis, MO); trehalose and sucrose were from Hayashibara Shoji Inc. (Okayama, Japan) and from Fluka Chemie AG (Buchs, Switzerland), respectively. The above products were used without further purification.

Received for publication 30 June 1998 and in final form 2 February 1999.

Address reprint requests to Lorenzo Cordone, Dipartimento di Scienze Fisiche ed Astronomiche, Via Archirafi, 36, 90123 Palermo, Italy. Tel.: 39 91 617 1708; Fax: 39 91 616 2461; E-mail: cordone@fisica.unipa.it.

© 1999 by the Biophysical Society

0006-3495/99/05/2727/08 \$2.00

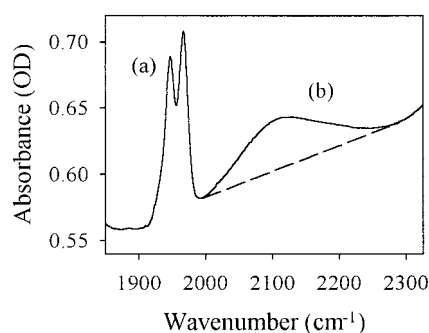


FIGURE 1 CO stretching bands in MbCO (a) and association band of water (b). Information on the water content was obtained by drawing the tangent between the two minima as shown. The data in the figure refer to the sample without sugar after ≈ 0.5 h of dehydration within the FTIR spectrometer (see Materials and Methods).

Measurements were performed at 25°C on a Biorad Digilab FTS-40A FTIR spectrometer with 2 cm^{-1} resolution. Samples were prepared by dissolving lyophilized ferric protein ($\approx 5 \cdot 10^{-3}$ M) in solutions containing $2 \cdot 10^{-1}$ M trehalose (or sucrose) and $2 \cdot 10^{-2}$ M phosphate buffer, pH 7. Solutions were centrifuged, equilibrated with CO, and reduced by anaerobic addition of sodium dithionite (10^{-1} M); 0.5 ml aliquots of the above solutions were layered on CaF₂ windows of 4.5 cm² surface and dried under a CO atmosphere in a silica gel desiccator. When samples were hard enough to stay in a vertical position (≈ 7 h at 25°C), the drying process was allowed to proceed inside the FTIR spectrometer, in a dry nitrogen atmosphere, while performing measurements. The nitrogen flux inside the spectrometer during the desiccation process was maintained constant at 5 l/min. The FTIR sample holder was modified in such a way to enable us to follow, alternatively, the dehydration process of both samples in a single run. The sample without sugar was prepared by the same procedure and dried under CO flux until it was hard enough to stay in a vertical position. We think it is most important to underline that the details of the results are highly dependent on experimental conditions, like detailed sample composition, temperature, and N₂ flux in the FTIR spectrometer.

Gravimetric determination of residual water after complete dehydration was performed by weighing a sample of known composition before starting desiccation (liquid phase) and after complete dehydration. Rehumidification of dry samples was performed in a box wherein humidity was controlled using a hygrotransmitter humidistat HD9217 (Delta Ohm, Padova, Italy).

The CO stretching bands were fitted in terms of three Voigtian bands (A substates: A₀, A₁, A₃) (Ansari et al., 1987), a Gaussian extrapolation taking into account the queue of the adjacent association band of water, and a constant term taking into account the increasing turbidity during the dehydration process (see below).

Fittings were performed by using a least-square Marquardt algorithm (Bevington and Robinson, 1992).

RESULTS AND DISCUSSION

Evolution of the samples during the first run of dehydration

In Fig. 2 a we report the area of the water association band as a function of desiccation time. We consider $t = 0$ the instant at which samples were put inside the FTIR spectrometer after ~ 7 h desiccation within the silica gel desiccator (see Materials and Methods). Fig. 2 a shows that the presence of sugar sizeably slows down the dehydration rate of the sample; moreover, at difference with the sample

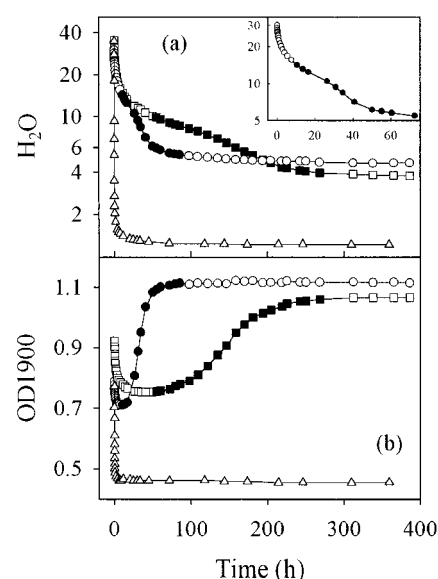


FIGURE 2 (a) Area of the association band of water (in OD · cm⁻¹, see text) and (b) optical density at 1900 cm⁻¹ (OD1900) as a function of desiccation time. \circ , Trehalose, \square , sucrose, \triangle , no sugar. Time 0 is the instant in which samples were put within the FTIR spectrometer after 7 h desiccation in a silica gel desiccator (see Materials and Methods). The inset in (a) shows the initial slowing and the following acceleration of dehydration rate in the trehalose-containing sample. Measurements were performed at 25°C. For the sake of comparison between (a) and (b), the data points relative to the microcrystallization process are shown by closed symbols.

without sugar, the dehydration rate of saccharide-containing samples shows three distinct behaviors: after an initial slowing down of the dehydration rate, a rate increase is evident (*closed symbols*); this second behavior is followed by a third one, wherein the dehydration rate is vanishing although water is still present in the samples. The acceleration evident in Fig. 2 a is paralleled by a turbidity increase detected by following the optical density at 1900 cm⁻¹ (OD1900), as a function of time. This frequency value lies on the queue of the water association band (Eisenberg and Kauzmann, 1969). Therefore, in the absence of a turbidity increase, it should always decrease during dehydration. On the contrary, Fig. 2 b shows that, in the saccharide-containing samples, the OD1900, after an initial decrease related to water extrusion, has a sizeable increase reflecting an upward translation of the whole band, indicative of a turbidity increase. The acceleration of the dehydration rate and the parallel turbidity increase are suggestive of microcrystal formation; in fact, microcrystals formation must bring about 1) extrusion of excess water from the crystalline structure, and 2) turbidity increase due to the scattering of incident light by microcrystals. In agreement with previous suggestions (Aldous et al., 1995) one can infer that the T_g value of the saccharide-protein complex is increased by the formation of microcrystals, incorporating traces of water and preventing water from acting as a "plasticizer" of the amorphous phase. In this respect it is worth noting that, at the end of the crystallization process, the amount of residual water

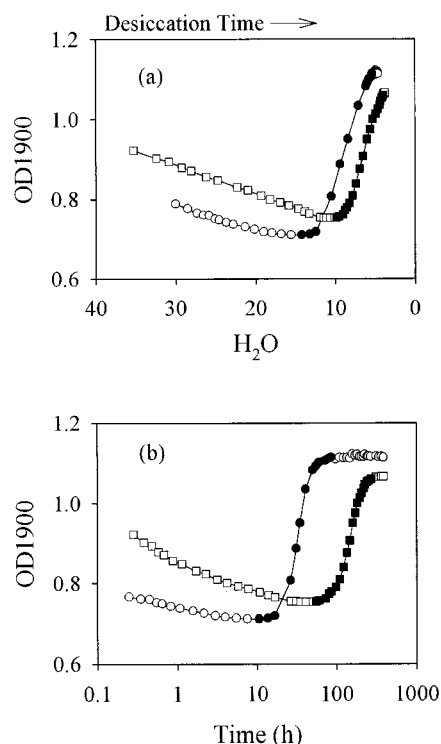


FIGURE 3 OD1900 as a function (a) of the area of the association band of water and (b) of the time in a logarithmic scale for trehalose- and for sucrose-containing samples. Symbols as in Fig. 2.

is slightly larger in the trehalose sample; moreover, gravimetric measurements indicated that at the end of microcrystallization the average residual water was ~ 2 water molecules per saccharide molecule in the trehalose sample and slightly lower in the sucrose sample.

A detailed discussion of the microcrystallization process in samples of different composition will be reported in a forthcoming paper; here we show how further interesting information is obtained from Fig. 3, *a* and *b*, where the OD1900 shown in Fig. 2 *b* is reported as a function of the samples' water content and as a function of time on a logarithmic scale. Fig. 3, *a* and *b* clearly indicate that the turbidity increase, evident in both saccharide-containing samples, reflects the same kind of process that in the two samples takes place in different time scales and at different water contents. The different behavior is likely due to dif-

ferences in the activation free energy of the process; in particular, we think that these differences are to be related to the higher symmetry of the trehalose molecule, which should bring about a lower activation entropy in the formation of the saccharide-protein-water microcrystals, and to the fact that trehalose molecules do not form direct internal hydrogen bonds between the two glucopyranose rings (see, e.g., Panek, 1995); both these points should enable crystallization at higher water content and in shorter times for the trehalose-containing sample.

Rehumidified samples

Overnight equilibration of dry samples with different ambient humidity resulted in water absorption. If rehumidified samples are put back in the FTIR spectrometer, a dehydration rate much larger than the one obtained in the first run, for equal water content, was observed, unless samples were equilibrated with a humidity $\geq 60\%$ for sucrose and $\geq 75\%$ for trehalose (see Fig. 4, *a* and *b*). In the latter cases the microcrystalline structure is lost, as evidenced also by the OD1900 value (see Fig. 5, *a* and *b*), and the dehydration process resulted to be almost identical to the one observed in the first run. For the sake of comparison between rehumidified samples, we think it is most relevant to stress that the two samples have been put in the humidifier and taken out together.

The behavior of rehumidified samples is indicative of a cooperative microcrystalline \rightarrow amorphous transition that takes place at suitable water content; we think the fact that trehalose remains in a microcrystalline structure up to higher rehumidification level than sucrose is most relevant. This might, in principle, be relevant in determining the differences between the two sugars in their action as bioprotectants.

Data in Fig. 5, *a* and *b* indicate that, although in rehumidified samples the OD1900 has the same behavior as in the first run, its absolute value is, for trehalose, sizeably higher when the sample is rehumidified at 40% and 60%; we attribute this finding to the fact that at these rehydration levels a reorganization of the microcrystalline structure takes place in trehalose, thus altering the microcrystal size and the sample turbidity.

FIGURE 4 Dehydration of rehumidified samples (at 25°C). The data of the first run are reported for comparison. (a) Trehalose; (b) sucrose. The humidity values at which rehumidified samples have been equilibrated are reported within the panels. For rehumidified samples the initial time was made to coincide with the time at which samples in the first run had analogous water content.

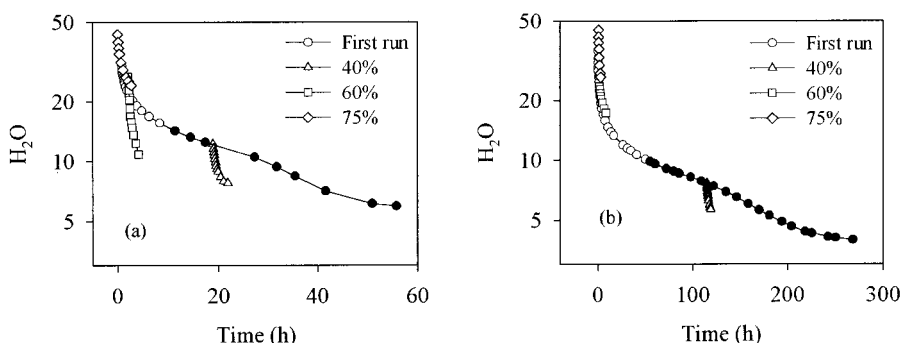
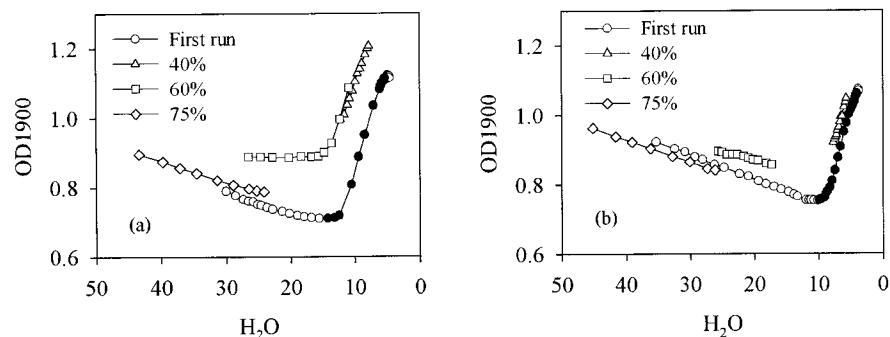


FIGURE 5 OD1900 as a function of water content for rehumidified samples. The data of the first run are reported for comparison. (a) Trehalose; (b) sucrose. The humidity values at which rehumidified samples have been equilibrated are reported within the panels.



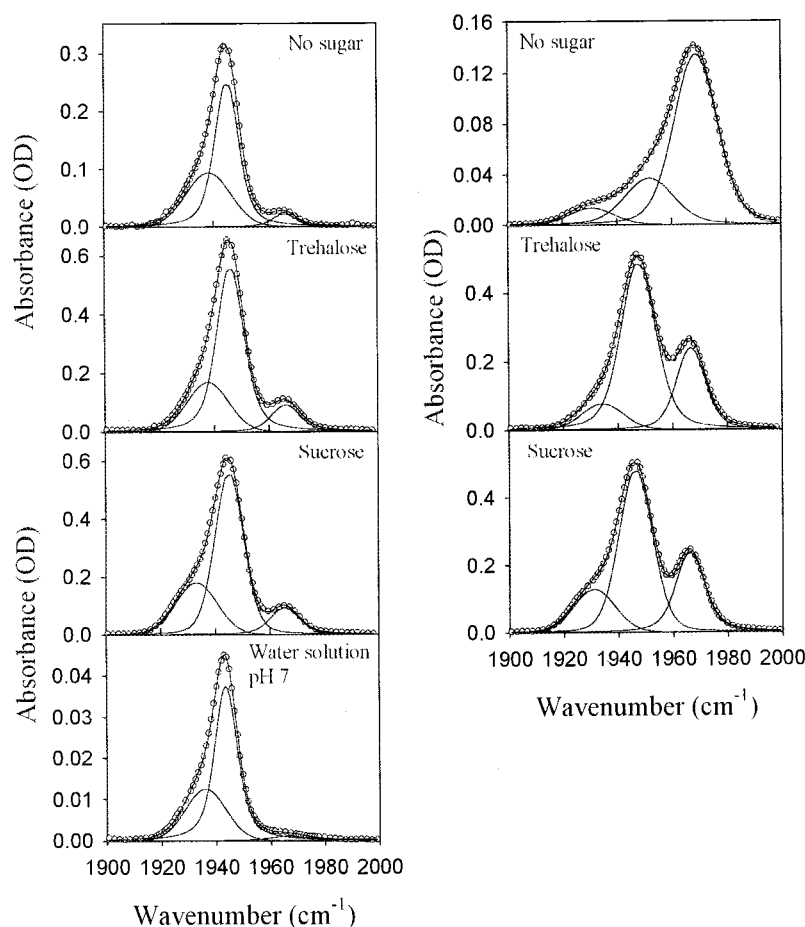
Effects of saccharide coating on the A substates of MbCO

In Fig. 6 we show the absorption of the CO stretching bands at $t = 0$ (most humid samples) and that of the driest samples, at the end of the first run of measurements. A sizeable decrease of bound CO is evident in the sample not containing sugar, where CO escape is prevented only following exhaustive dehydration; at variance, no CO escape is evident in saccharide-containing samples, even in the most humid amorphous phase.

To avoid noise in the parameters shown in Figs. 8–10 we proceeded to fit the data as follows: we first fitted the experimental data points leaving all the fitting parameters

free; this resulted in very high-quality fittings for each single spectrum. However, the evolution of the parameters obtained was rather noisy due to the low resolution of some A bands (see Fig. 6), to the interplay, in the Voigtians, between the Lorentzian and Gaussian width (Γ and σ , respectively), and to the variation of the Gaussian extrapolation during the dehydration process. For this reason we performed a further fitting wherein the values of all the Lorentzian widths Γ and of some Gaussian width σ (i.e., the less resolved parameters) were kept constant and fixed to given values, based on the outcome of the first fitting; this resulted again in very high-quality fittings (as shown in Fig. 6), with slightly larger residuals (Fig. 7). The evolution of

FIGURE 6 CO stretching bands (A substates) of MbCO at the beginning (left) and at the end (right) of our measurements. The Gaussian extrapolation taking into account the queue of the adjacent association band of water has been subtracted. Note that, due to the CO release and formation of ferric myoglobin in the sample without sugar, the area under the CO stretching bands has a large decrease during the measurements; such an effect is not found in saccharide-containing samples, where the above area exhibited an increase of $\approx 10\%$ during the dehydration process; we ascribe this effect to a variation of the oscillator strength relative to the A substates, due to the hardening of the matrix (Ansari et al., 1987). The low value of the area under the CO stretching bands in the sample without sugar and the further CO release during rehumidification did not allow us to perform meaningful measurements of rehumidified samples in the absence of saccharide.



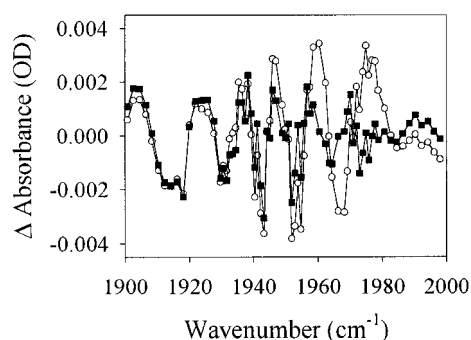


FIGURE 7 Residuals of the fittings for the driest trehalose sample; *closed symbols*: fitting with all parameters left free to vary; *open symbols*: fitting with constraints. Note that in this case the differences between the residuals obtained in the two kinds of fittings are the largest; much lower differences were typically obtained.

the parameters obtained is shown in Figs. 8–10; as it can be seen, almost no noise is present. In Table 1 are reported the values of parameters that were kept constant and, for comparison, the maximum and minimum value obtained in the fitting without constraints; these parameters were kept at the same values in the fitting of data relative to the first run of dehydration and to rehumidified samples.

First we shall discuss the evolution of parameters in the first run of dehydration: data in Figs. 8–10 indicate that water withdrawal has the same kind of effect on all the

parameters of all samples studied, although the particular values of the parameters are sample-dependent. Data in Figs. 8–10 show that in the absence of saccharide the effects of dehydration are much more pronounced, thus indicating that the saccharide matrix protects the protein against excessive structure deformation. Interestingly, the transition toward a crystalline matrix seems not to have dramatic effects on the evolution of the parameters that characterize the A substates.

An unambiguous finding evident in all samples is that water withdrawal sizeably increases the fraction of the A_0 substate (see e.g., Brown et al., 1983); this substate has been thought to correspond to MbCO molecules having the distal histidine out of the heme pocket and exposed to the solvent (Morikis et al., 1989); indeed, this substate is very sparsely populated at neutral pH (due to hydrophobic interaction), while it is highly populated at low pH, due to the histidine protonation (Ansari et al., 1987; Morikis et al., 1989). The large A_0 increase shown in Fig. 8 therefore suggests that in the absence of hydrophobic forces (due to the lack of bulk solvent) the MbCO conformations are sizeably displaced toward those having the distal histidine out of the heme pocket. Moreover, the amount of A_0 is much larger in the sample not containing sugar, wherein protein-protein contacts are more likely than in saccharide-containing samples; this might indicate that direct contacts among MbCO molecules might play a role in keeping the distal histidine out of

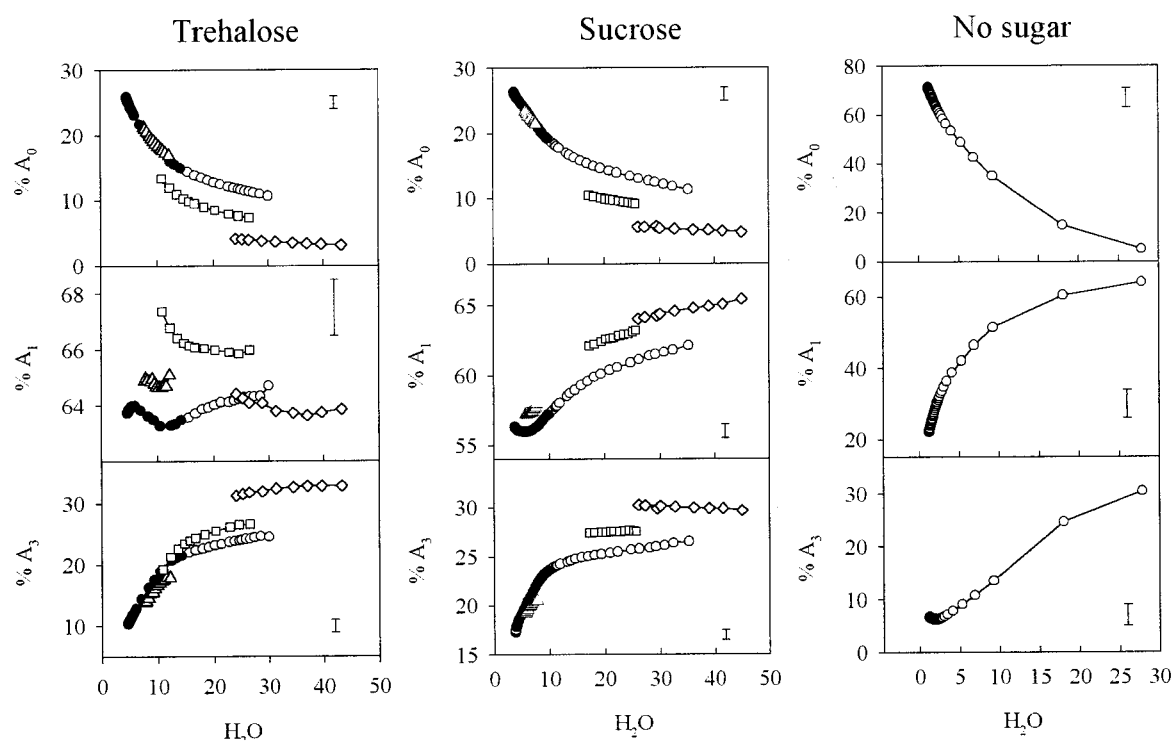


FIGURE 8 Population of A substates as a function of water content: data points represented by circles refer to the first run of dehydration. \circ , Before and at the end of microcrystallization; \bullet , during microcrystallization (see Figs. 2 and 3); \triangle , samples rehumidified at 40% relative humidity; \square , samples rehumidified at 60% relative humidity; \diamond , samples rehumidified at 75% relative humidity. Note the sizeable decrease of A_0 and the increase of A_3 in saccharide-containing samples following rehumidification at 75%. Error bars derived from data reproducibility are shown.

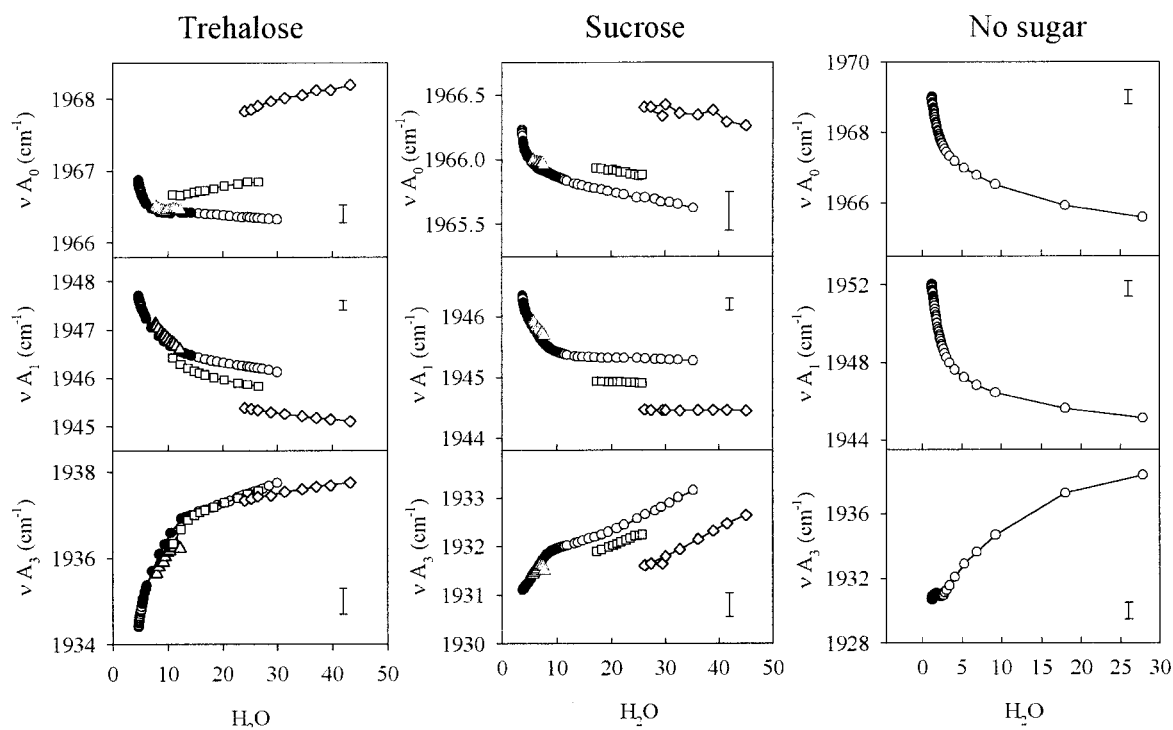


FIGURE 9 Peak frequency values of A substates population as a function of water content. Symbols as in Fig. 8.

the heme pocket in dry protein. The role played by direct protein-protein contacts is also suggested by the extremely large broadening present in the A_0 and A_1 substates in the sample without sugar (Fig. 10).

As shown in Figs. 8–10, if samples are rehumidified at low humidity (40%), the distribution of A substates and of the relative parameters is barely distinguishable from the one observed in the first run of dehydration; at variance,

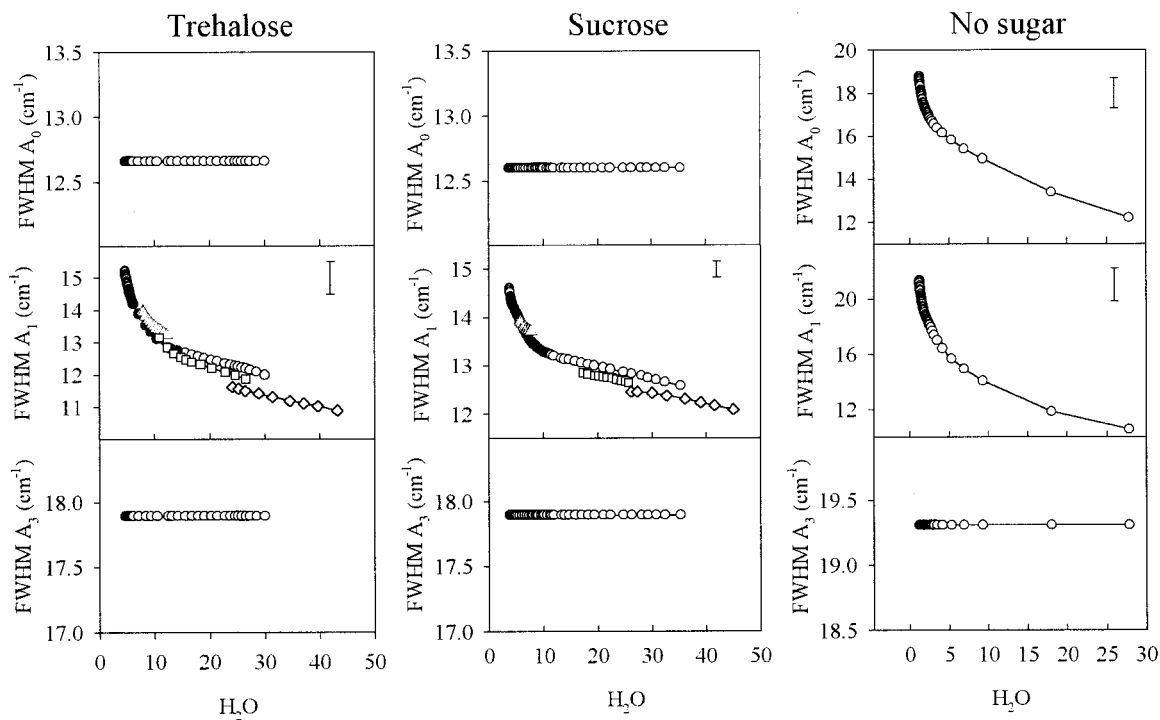


FIGURE 10 Bandwidth values relative to A substates as a function of water content. Symbols as in Fig. 8. Note that, as mentioned in the text, some values have been held constant to avoid noise in the resulting fitting parameters.

TABLE 1 Values of Lorentzian (Γ) and Gaussian (σ) width used in the fittings with constraints

	A_0	A_1	A_3
No sugar	$\Gamma = 1.9^*$ σ Free	$\Gamma = 2.3^*$ σ Free	$\Gamma = 0^{\#}$ $\sigma = 8.2$ [7.5 ÷ 9.0]
Trehalose	$\Gamma = 2.0$ [1.6 ÷ 2.5] $\sigma = 4.4$ [4.1 ÷ 4.6]	$\Gamma = 2.5$ [2.1 ÷ 2.9] σ Free	$\Gamma = 0^{\#}$ $\sigma = 7.6$ [7.2 ÷ 8.1]
Sucrose	$\Gamma = 2.5$ [2.0 ÷ 3.2] $\sigma = 4.1$ [3.9 ÷ 4.2]	$\Gamma = 1.1$ [0.9 ÷ 1.3] σ Free	$\Gamma = 0^{\#}$ $\sigma = 7.6$ [7.4 ÷ 8.0]

Maximum and minimum values obtained in the fitting without constraints are shown in brackets.

*Due to the fact that in samples without sugar some substates are very little resolved, a rather large interplay between Γ and σ was observed in fittings without constraints; therefore, for samples not containing sugar, Γ was fixed at the values obtained under the conditions where this parameter was better resolved, i.e., Γ (A_1) was fixed at the value obtained in the most humid sample; Γ (A_0) was fixed at the value obtained in the driest sample.

[#]In agreement with previously reported data (Mayer, 1994) the A_3 substate was always found to be purely Gaussian, i.e., $\Gamma = 0$.

sizeable effects on the distribution of A substates (Figs. 8–10) and on the relative parameters are seen for larger rehumidification levels (60% and 75%). This suggests that during the first dehydration run, the saccharide matrix forces the protein within a stressed conformation which, following the addition of water molecules, relaxes toward structures different from those present during the first run of dehydration at equal water content. In particular, a sizeable decrease in the population of the A_0 substate with respect to the one observed in the presence of an analogous water content in the first run of dehydration, is evident in samples rehumidified at 75% relative humidity. This suggests 1) that in these samples the distal histidine is again inside the heme pocket and 2) that there is not one to one correspondence between the protein structure (as reflected in the A substates) and sample water content.

Further studies are needed for fully rationalizing the mechanisms through which the water-saccharide matrix influences the protein structure and, in particular, the A substates at the microscopic level.

CONCLUSIONS

Sample dehydration and crystallization

As mentioned in the Introduction, the properties that make trehalose unique with respect to other saccharides for preservation of dry biomaterials are still poorly understood. In agreement with previous suggestions (Aldous et al., 1995), the presently reported results indicate that the saccharide-protein glasses can be stabilized by incorporating traces of water into a crystalline structure, thus preventing water from acting as a “plasticizer” of the amorphous state and increasing the glass transition temperature (T_g) of the system

(Green and Angell, 1989; Crowe et al., 1996). In the trehalose-containing sample, this crystallization process takes place in a shorter time scale and at larger water content than in the sucrose-containing sample. Moreover, the behavior of rehumidified samples indicates that in both saccharides, the crystalline structure is lost following equilibration with a suitable humidity level that is higher for the trehalose-containing sample. We suggest that the behavior of trehalose samples in the amorphous \rightarrow microcrystal and microcrystal \rightarrow amorphous transition may be most relevant in determining the peculiarity of this sugar as bioprotectant.

Saccharide-coated MbCO

Protein dynamics are sizeably different at low and high temperature (Parak et al., 1986; Doster et al., 1989; Di Pace et al., 1992); in fact, while harmonic modes dominate the low-temperature behavior (Melchers et al., 1996), additional nonharmonic motions occur above ~ 180 K. These motions, typical for proteins, are often called *protein-specific motions*; they reflect thermal fluctuations of a molecule among protein substates (Frauenfelder et al., 1988) and are a prerequisite for protein function.

Embedding MbCO in dry trehalose glasses hinders large-scale protein-specific motions (Hagen et al., 1995, 1996; Gottfried et al., 1996; Cordone et al., 1998, 1999); this avoids the escape of CO from the heme pocket at room temperature also after prolonged illumination. The presently reported results indicate that in saccharide-coated MbCO the CO escape is prevented also in samples that are in a most humid amorphous phase. This finding indicates that some inhibition of protein-specific motions takes place even in the most humid samples (Kleinert et al., 1998). At variance, the CO escape is not prevented in MbCO dried in the absence of sugar, unless exhaustive dehydration is reached, thus indicating that in the absence of sugar, protein-specific motions enabling the CO escape are hindered only in extremely dry protein.

Inhibition of protein-specific motions, as detected by Mössbauer spectroscopy, has also been observed for fully dried myoglobin in the absence of sugar (Parak et al., 1986); however, as shown by the presently reported results, large differences in the heme pocket structure (as shown by the evolution of A substates) are evident between the saccharide-coated protein and the protein dried in the absence of sugar.

The effects of trehalose coating on the CO recombination after flash photolysis in heme proteins have been reported (Hagen et al., 1995, 1996; Gottfried et al., 1996); the authors showed that some part of protein dynamics is strongly inhibited. In light of the present data on the evolution of A substates in saccharide-coated MbCO it seems most relevant to perform analogous measurements, as well as the Mössbauer, optical, and neutron-scattering ones (Cordone et al., 1998, 1999) in saccharide-coated samples having different “history.” This would shed light on the effects of the

rigidity of the surrounding matrix and of its water content on protein specific motions and in particular on protein relaxation. In fact, we think that an "inverse water effect" similar to the "inverse temperature effect" (Friedman, 1985; Nienhaus et al., 1992; Sastry and Agmon, 1997) should be evidenced by performing measurements of recombination after flash photolysis in saccharide-coated samples of increasing water content.

We thank R. Carrotta, O. Comite, A. Cupane, S. Fornili, M. Leone, S. Micciancio, M. U. Palma, P. L. San Biagio, and M. B. Vittorelli for useful discussions and criticisms. The technical assistance of F. D'Anca, G. Lapis, and G. Tricomi is gratefully acknowledged.

This work was co-financed by the European Community (European Funds for Regional Development).

REFERENCES

- Aldous, B. J., A. D. Auffret, and F. Franks. 1995. The crystallization of hydrates from amorphous carbohydrates. *Cryo-letters* 16:181–186.
- Ansari, A., J. Berendzen, D. Braunstein, B. R. Cowen, H. Frauenfelder, M. K. Hong, I. E. T. Iben, J. B. Johnson, P. Ormos, T. B. Sauke, R. Scholl, A. Schulte, P. J. Steinbach, J. Vittitow, and R. D. Young. 1987. Rebinding and relaxation in the myoglobin pocket. *Biophys. Chem.* 26:337–355.
- Bevington, P. R., and D. K. Robinson. 1992. Data reduction and error analysis for the physical sciences. 2nd ed. McGraw-Hill, New York. 161–164.
- Brown, W. E., J. W. Sutcliffe, and P. D. Pulsinelli. 1983. Multiple internal reflectance infrared spectra of variably hydrated hemoglobin and myoglobin films: effects of globin hydration on ligand conformer dynamics and reactivity at the heme. *Biochemistry* 22:2914–2923.
- Caughey, W. S., H. Shimada, G. C. Miles, and M. P. Tucker. 1981. Dynamic protein structures: infrared evidence for four discrete rapidly interconverting conformers at the carbon monoxide binding site of bovine heart myoglobin. *Proc. Natl. Acad. Sci. USA* 78:2903–2907.
- Cordone, L., P. Galajda, E. Vitranò, A. Gassmann, A. Ostermann, and F. Parak. 1998. A reduction of protein specific motions in co-ligated myoglobin embedded in a trehalose glass. *Eur. Biophys. J.* 27:173–176.
- Cordone, L., M. Ferrand, E. Vitranò, and G. Zaccari. 1999. Harmonic behavior of trehalose-coated carbonmonoxy-myoglobin at high temperature. *Biophys. J.* 76:000–000.
- Crowe, L. M., D. S. Reid, and J. H. Crowe. 1996. Is trehalose special for preserving dry biomaterials? *Biophys. J.* 71:2087–2093.
- Di Pace, A., A. Cupane, M. Leone, E. Vitranò, and L. Cordone. 1992. Vibrational coupling, spectral broadening mechanisms, and anharmonicity effects in carbonmonoxy heme proteins studied by the temperature dependence of the Soret band lineshape. *Biophys. J.* 63:475–484.
- Doster, W., S. Cusack, and W. Petry. 1989. Dynamical transition of myoglobin revealed by inelastic neutron scattering. *Nature* 337:754–756.
- Eisenberg, D., and W. Kauzmann. 1969. The structure and properties of water. Oxford University Press, London. 228–231.
- Frauenfelder, H., N. A. Alberding, A. Ansari, D. Braunstein, B. R. Cowen, M. K. Hong, I. E. T. Iben, J. B. Johnson, S. Luck, M. C. Marden, J. R. Mourant, P. Ormos, L. Reinish, R. Scholl, A. Schulte, E. Shyamsunder, L. B. Sorensen, P. J. Steinbach, A. H. Xie, R. D. Young, and K. T. Yue. 1990. Proteins and pressure. *J. Phys. Chem.* 94:1024–1037.
- Frauenfelder, H., F. Parak, and R. D. Young. 1988. Conformational substates in proteins. *Annu. Rev. Biophys. Biophys. Chem.* 17:451–479.
- Frauenfelder, H., S. G. Sligar, and P. G. Wolynes. 1991. The energy landscapes and motions of proteins. *Science* 254:1598–1603.
- Friedman, J. M. 1985. Structure, dynamics and reactivity in hemoglobin. *Science* 228:1273–1280.
- Gottfried, D. S., E. S. Peterson, A. G. Sheikh, J. Wang, M. Yang, and J. M. Friedman. 1996. Evidence for damped hemoglobin dynamics in a room temperature trehalose glass. *J. Phys. Chem.* 100:12034–12042.
- Green, J. L., and C. A. Angell. 1989. Phase relations and vitrification in saccharide-water solutions and trehalose anomaly. *J. Phys. Chem.* 93:2880–2882.
- Hagen, S. J., J. Hofrichter, and W. A. Eaton. 1995. Protein reaction kinetics in a room-temperature glass. *Science* 269:959–962.
- Hagen, S. J., J. Hofrichter, and W. A. Eaton. 1996. Geminate rebinding and conformational dynamics of myoglobin embedded in a glass at room temperature. *J. Phys. Chem.* 100:12008–12021.
- Kleinert, T., W. Doster, H. Leyser, W. Petry, V. Schwarz, and M. Settles. 1998. Solvent composition and viscosity effects on the kinetics of CO binding to horse myoglobin. *Biochemistry* 37:717–733.
- Leslie, S. B., E. Israeli, B. Lighthart, J. H. Crowe, and L. M. Crowe. 1995. Trehalose and sucrose protect both membranes and proteins in intact bacteria during drying. *Appl. Environ. Microbiol.* 61:3592–3597.
- Makinen, M. W., R. A. Houtchens, and W. S. Caughey. 1979. Structure of carboxymyoglobin in crystals and in solution. *Proc. Natl. Acad. Sci. USA* 76:6042–6046.
- Mayer, E. 1994. FTIR spectroscopic study of the dynamics of conformational substates in hydrated carbonyl-myoglobin films via temperature dependence of the CO stretching band parameters. *Biophys. J.* 67:862–873.
- Melchers, B., E. W. Knapp, F. Parak, L. Cordone, A. Cupane, and M. Leone. 1996. Structural fluctuations of myoglobin from normal modes, Mössbauer, Raman, and absorption spectroscopy. *Biophys. J.* 70:2092–2099.
- Morikis, D., P. M. Champion, B. A. Springer, and S. G. Sligar. 1989. Resonance Raman investigation of site-directed mutants of myoglobin: effects of distal histidine replacement. *Biochemistry* 28:4791–4800.
- Mourant, J. R., D. P. Braunstein, K. Chu, H. Frauenfelder, G. U. Nienhaus, P. Ormos, and R. D. Young. 1993. Ligand binding to heme proteins. II. Transitions in the heme pocket of myoglobin. *Biophys. J.* 65:1496–1507.
- Nienhaus, G. U., J. R. Mourant, and H. Frauenfelder. 1992. Spectroscopic evidence for conformational relaxation in myoglobin. *Proc. Natl. Acad. Sci. USA* 89:2902–2906.
- Panek, A. D. 1995. Trehalose metabolism: new horizons in technological applications. *Braz. J. Med. Biol. Res.* 28:169–181.
- Parak, F., M. Fischer, E. Graffweg, and H. Formanek. 1986. Distribution and fluctuations of protein. In *Structure and Dynamics of Nucleic Acids, Proteins and Membranes*, E. Clementi and S. Chin, editors. Plenum Press, New York. 139–148.
- Prestrelski, S. J., N. Tedeschi, T. Arakawa, and J. F. Carpenter. 1993. Dehydration-induced conformational transitions in proteins and their inhibitions by stabilizers. *Biophys. J.* 65:661–671.
- Sastry, G. M., and N. Agmon. 1997. Trehalose prevents myoglobin collapse and preserves its internal mobility. *Biochemistry* 36:7097–7108.
- Uritani, M., M. Takai, and K. Yoshinaga. 1995. Protective effect of disaccharides on restriction endonucleases during drying under vacuum. *J. Biochem.* 117:774–779.